THE REDUCED BEAM SECTION MOMENT CONNECTION WITHOUT CONTINUITY PLATES

Scott M. ADAN[1] and Lawrence D. REAVELEY[2]

SUMMARY

The reduced beam section (RBS) beam-to-column moment connection was tested without the use of continuity plates at the University of Utah. Four full-scale tests were performed, each closely following the protocols established for stepwise increasing cyclic tests published by the SAC Steel Project. The tests concluded the connections were able to meet and exceed the plastic joint rotation requirements for special moment frames without the use of the continuity plates. Following the tests, nonlinear finite element models of the same connections were created using the computer program, ANSYS. The nonlinear modeling established a correlation to the tested specimens and included buckling behavior. With this correlation, the mechanics of the connections were subject to further study. The purpose of the testing and subsequent study is to establish a design procedure for using the RBS beam-to-column moment connection without continuity plates. By eliminating the continuity plates, material and labor cost reductions can provide an economic benefit to steel moment frame construction.

INTRODUCTION

Following the 1994 Northridge earthquake, a significant amount of research activity was initiated on the behavior of fully restrained steel connections. Much of the research has focused on the Reduced Beam Section (RBS) moment connection. The RBS connection utilizes a circular radius cut in both top and bottom flanges to reduce the flange area and therefore the plastic moment capacity over a length of the beam near the ends of the beam span. This connection was developed to assure greater reliability of steel beam-to-column connections. The notion behind the connection is to protect against dynamic overloading of connection welds through an intentional ductile "fuse".

Continuity plates have been an integral part of nearly all code pre-qualified steel moment connections including the RBS. These stiffeners, positioned horizontally on each side of the column web, provide a

---

[1] Project Manager, KPFF Consulting Engineers, 1601 Fifth Ave., Suite 1600, Seattle, WA. Email: scott.adan@kpff.com
[2] Professor and Chair, Department of Civil and Environmental Engineering, University of Utah, Salt Lake City, UT. Email: lreaveley@civil.utah.edu

continuous load path between the beam flange and the column web. However, the absolute necessity of continuity plates in RBS moment connections is clouded in uncertainty.

In prior testing at the University of Utah, four full-scale RBS moment connection specimens were evaluated in accordance with the SAC Steel Project [1] stepwise cyclic protocols, each without the use of continuity plates. The four test specimens consisted of two matched pairs of columns and beams. One pair of the tested specimens performed adequately; the other pair performed adequately but appeared to be at a point of instability, Okahshi [2]. All the specimens exhibited lateral-torsional buckling behavior when subjected to high degrees of angular rotation.

In an effort to gain additional insight into the behavior of the tested specimens, the study was broadened to include creation of nonlinear finite element models. The study uses a general-purpose finite element modeling program, ANSYS/Multiphysics, to perform a series of nonlinear finite element analyses. The finite element analyses were able to correlate both nonlinear behavior and lateral-torsional-buckling as observed during testing of specimens in the laboratory. Select results of the both the laboratory testing and the finite element analyses are summarized in this paper.

RBS MOMENT CONNECTION TESTING PROGRAM

Test Specimens

Four full-scale tests were performed on the moment connection using the RBS, each closely following the protocols established for stepwise increasing cyclic tests published by the SAC Steel Project [1]. All four tests were performed with a beam size of W30x132. The beams were paired up W14x283 and W18x211 columns. The specimens are designated as RBS1 through RBS4. The specimen sizes, steel grades, mill certificates, and coupon data are shown in Table 1.

Table 1: Beam and column specimen parameters.

Specimen #	Member	Size	Grade	Mill Certificate		Coupon Data	
				Yield Stress (ksi)	Ultimate Stress (ksi)	Yield Stress (ksi)	Ultimate Stress (ksi)
RBS1	Beam	W30x132	A572 Gr 50	55.0	73.0	55.6	74.1
	Column	W14x283	A572 Gr 50	51.0	74.0	56.3	78.5
RBS2	Beam	W30x132	A572 Gr 50	55.0	73.0	55.6	74.1
	Column	W14x283	A572 Gr 50	51.0	74.0	56.3	78.5
RBS3	Beam	W30x132	A572 Gr 50	55.0	73.0	55.6	74.1
	Column	W18x211	A572 Gr 50	53.0	70.0	51.8	70.3
RBS4	Beam	W30x132	A572 Gr 50	55.0	73.0	55.6	74.1
	Column	W18x211	A572 Gr 50	53.0	70.0	51.8	70.3

The reduced sections were cut from the beam flanges in a 21 inch circular radius. In each case, approximately 40 percent of the beam flange width was removed. The beam web and flanges were connected to the column flange with a complete joint penetration groove weld. All groove welds were made with a self-shielded flux cored arc welding process using an E71T-8 electrode. The E71T-8 provides a minimum specified Charpy V-Notch (CVN) value of 20 foot-pounds at -20 degrees Fahrenheit. No continuity plates were installed.

Test Setup and Procedure

The test set-up was configured to represent a condition where the beam supports a slab and is in direct contact with the slab along the length of the beam top flange. As shown in Fig. 1, vertical elements were positioned on each side of the beam to brace the beam top flange. The test specimens were all fitted with the full instrumentation recommended by SAC [1]. Instrumentation devises included strain gages, load cells, and displacement transducers. Special attention was placed on measuring the displacements associated with various points along the welded column flanges. In addition, portions of the connection were whitewashed to record visuals sign of induced stress.

Fig. 1: RBS moment connection specimen test set-up.

Each of the test specimens were subject to a displacement controlled loading history based on the protocol recommended by SAC [1] at rate of 2 inches per minute. The applied number of load cycles, inter-story drift angles, and beam end displacements are shown in Table 2.

Table 2: Load Cycle Schedule.

| Load Step #	Total Inter-story Drift Angle (radian x 10^{-3})	Number of Load Cycles	Beam End Displacement (inch)
1	0.375	6	±0.64
2	0.5	6	±0.84
3	0.75	6	±1.26
4	1.0	4	±1.68
5	1.5	2	±2.52
6	2.0	2	±3.35
7	3.0	2	±5.03
8	4.0	2	±6.70
9	5.0	2	±8.40

Test Results

The test performance of each of the four specimens was similar. Initial yielding was visually observed during load step #4. Whitewash flaking initiated in the beam web, near the thinnest section of the reduced flange. As indicated in Fig. 2, the flaking progressed across the entire beam web and initiated in the column panel zone. At load step #6, localized buckling of the beam web occurred in the flaking areas. With each subsequent downward cycle, lateral torsional buckling occurred in the beam bottom flange. As

shown in Fig. 3, the lateral torsional buckling mode twisted the bottom flange outward. At load step #8, localized buckling of the beam occurred in the reduced flange. At load higher load steps, severe web buckling was observed in the beam web (Fig. 4) and on the upward cycles, buckling was also observed in the beam top flange.
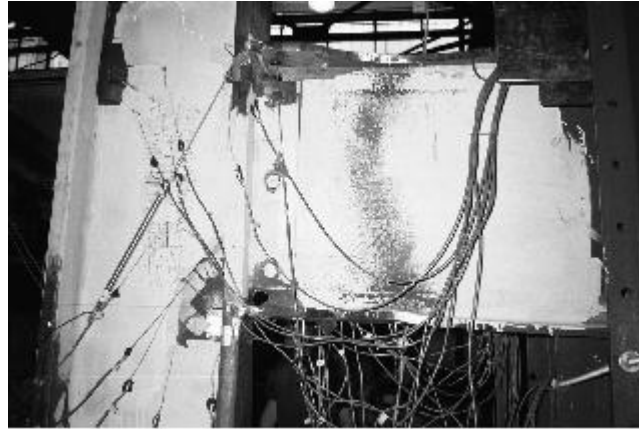
Fig. 2: Observed whitewash flaking in the RBS and column panel zone.
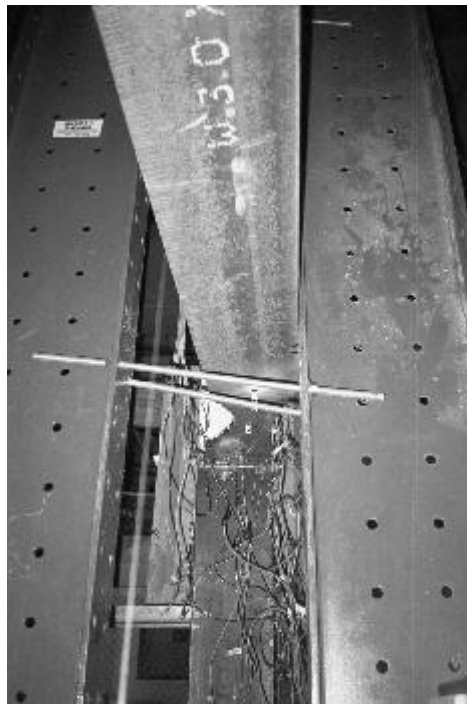
Fig. 3: Observed lateral torsional buckling looking below the test specimen.
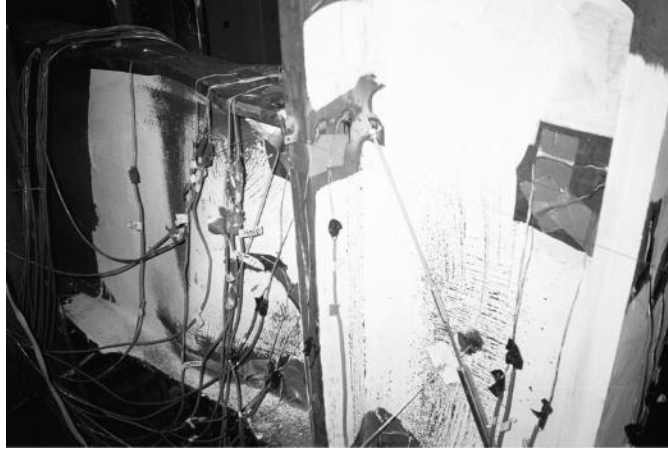
Fig. 4: Localized beam web buckling and beam bottom flange deformation.

Ultimately, all specimens fractured shortly after load step #9. Fractures initiated during the return from the downward load cycle in the thinnest section of the beam bottom flange where previous localized flange buckling had been observed. There was no significant weld damage in any of the beam-to-column welds. No evidence of weld failure was observed in any of the tests.

The tests concluded that for these specimens, the connections were able to meet and exceed the plastic rotation connection demand requirements required by SAC [1] for special moment frames, without the use of continuity plates.

INVESTIGATION USING FINITE ELEMENT ANALYSIS

Finite Element Parameters
In an effort to gain additional insight into the nonlinear and buckled behavior of the tested specimens, the study was broadened to include creation of finite element models. The study uses a general-purpose finite element modeling program, ANSYS/Multiphysics, to perform a series of nonlinear finite element analyses. The modeling considers beam web buckling which was seen to trigger lateral torsion buckling of the beam bottom flange.

The finite element models are comprised of four node, three-dimensional shell elements. The selected element is the SHELL181 by ANSYS [3]. This element is defined by four nodes, four thicknesses, and the orthotropic material properties. The element has six degrees of freedom at each node: translations in the nodal x, y, and z directions and rotations about the nodal x, y, and z axes. The element has plasticity, creep, stress stiffening, large deflection, and large strain capabilities.

The element accounts for material nonlinearities through classical metal plasticity theory based on the von Mises yield criterion. Geometric nonlinearities are accounted for through a small strain, large displacement formulation. Isotropic hardening is assumed for the monotonic analyses. Furthermore, because the analysis is for monotonic loading conditions, it is assumed that conclusions drawn from this work are qualitatively applicable to cyclic conditions.

The modeling does not address the issue of fracture propagation. The study is concerned with the potential for cracking only through the development of stress and strain states that would facilitate fracture if a flaw or other irregularity were introduced.

Material Properties

All the column and beam specimens were reported to be ASTM A572 grade 50/ A992 steel (see Table 1). Upon completion of the physical testing, tensile coupons were prepared and mechanically tested to the procedures of ASTM A6, A370. Fig. 5, 6, and 7 illustrate the stress versus strain curves from the tensile coupon tests for the W14x283 column, the W18x211 column and the W30x132 beam, respectively. Four tensile coupon tests were preformed for each member. Two samples were extracted from the beam flange and two in the beam web. In the computer modeling, the matching multi-linear stress strain curves were input directly as element material properties.
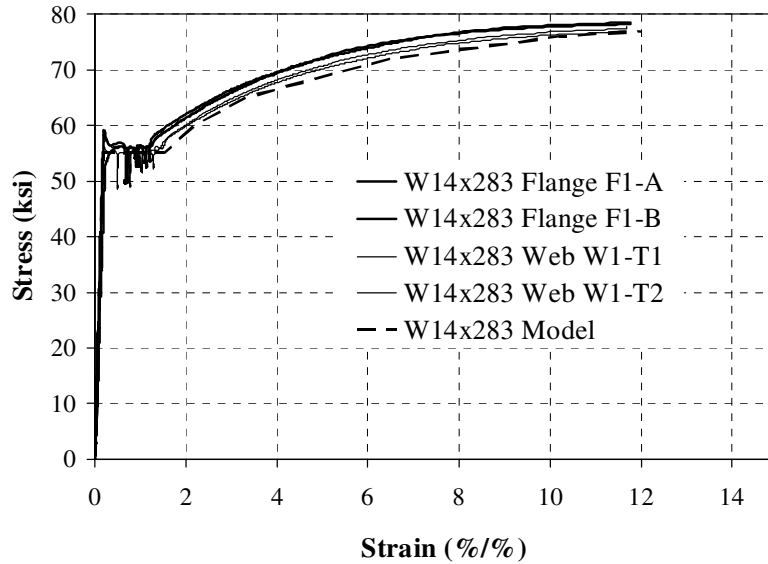
Fig. 5: Stress versus strain curves for the W14x238 column.
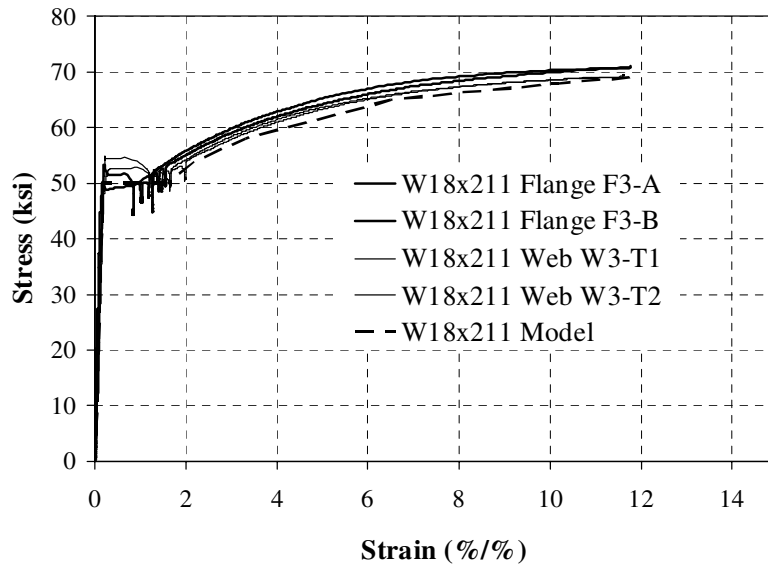

Fig. 6: Stress versus strain curves for the W18x211 column.
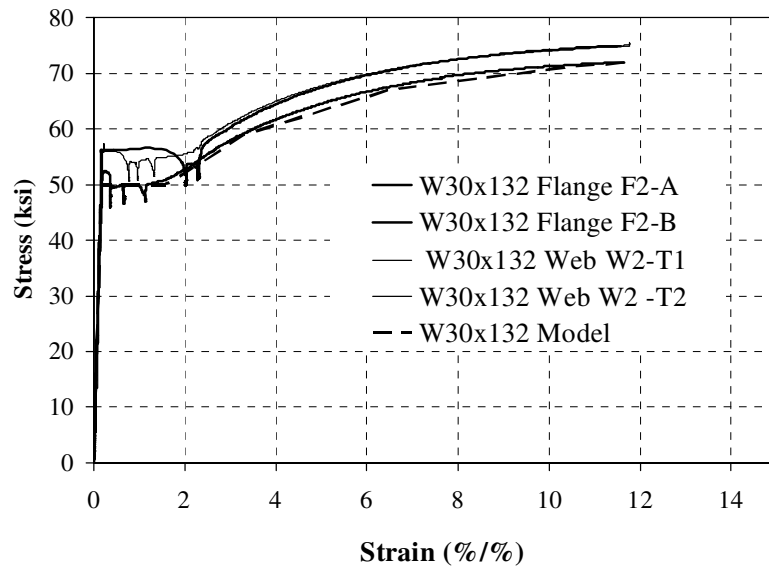
Fig. 7: Stress versus strain curves for the W30x132 beam.

Modeling Considerations

On the tested specimens, the beam web and flanges were fully restrained to the column flange with full penetration welds. In the computer model, the beam to column element connection is also configured as being fully restrained. Curved weld access holes are simplified to permit a relatively coarse mesh configuration around the circumference of the hole. The meshed model for RBS1 (W14x283 column) specimens is shown in Fig. 8. The meshed model for the RBS3 (W18x211 column) is similar but in the interest of preserving space, is not shown.
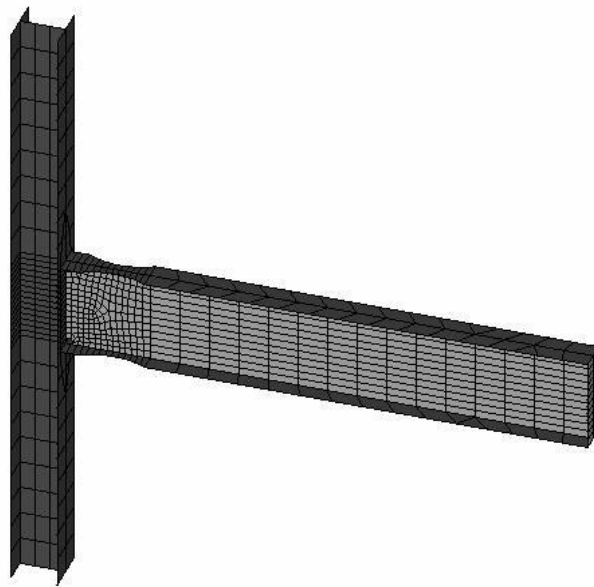
Fig. 8: Oblique view of the RBS1 (W14x283 column) finite element model.

Boundary conditions are applied to the models to match that of the tested connections. The columns are pinned at the base and at the top. The beam top flange is laterally restrained at both 40 inches and 136 inches from the column centerline. The beam bottom flange is laterally restrained at 136 inches from the column centerline. Beam vertical translation is applied 168 inches from the column centerline to simulate the actuator attachment. The computer model was subjected to the same incremental loading history as shown in Table 2, although the number of cycles in each load step was limited to one.

As indicated in Fig. 3, a characteristic lateral-torsional mode of beam buckling was observed during testing. This mode of buckling is difficult to simulate using computer modeling. However, the nonlinear analyses were able to consider beam web and lateral torsional buckling by employing a sophisticated technique of expanding an eigenvalue buckling analysis into the nonlinear solution of the model.

An eigenvalue buckling analysis predicts the theoretical buckling strength (the bifurcation point) of an ideal linear elastic structure. This method corresponds to the textbook approach to elastic buckling analysis. For example, an eigenvalue buckling analysis of a column will match the classical Euler solution.

Generally speaking, if the loading on the computer elements are perfectly in-plane (that is, flexural or axial stresses only), the out-of-plane defections necessary to initiate buckling will not develop, and the analysis will fail to predict buckling behavior. To overcome this problem, a preliminary eigenvalue buckling analysis is expanded into the solution to create the onset of small out-of-plane perturbations.

Fig. 9 illustrates the eigenvalue elastic buckling mode shape for the RBS1 (W14x283 column) specimen. The darker colored contoured areas are included to highlight location on the beam and column experiencing higher degrees of rotation. As with that of the tested connections, the beam appears in the classical lateral torsional buckling shape.
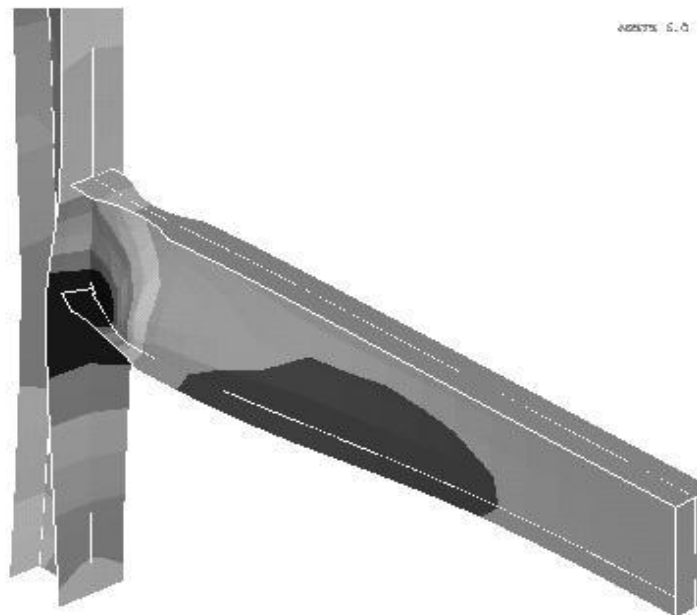

**Fig. 9: Isometric view of the RBS1 (W14x283 column) elastic buckling mode shape.**

Validation of the Finite Element Modeling
The finite element modeling was verified by comparing the measured cyclic responses of the tested specimens with the computed response.

Fig. 10 and 11 show the comparisons of the moment versus plastic rotation for RBS1 (W14x283 column) and RBS3 (W18x211 column) specimens, respectively. The plastic rotation was obtained by subtracting the elastic rotation from the total inter-story drift angle Uang [4]. As expected, the hysteretic curves for RBS2 and RBS4 were similar to those of RBS1 and RBS3. In the interest of preserving space, they are not included in this paper.
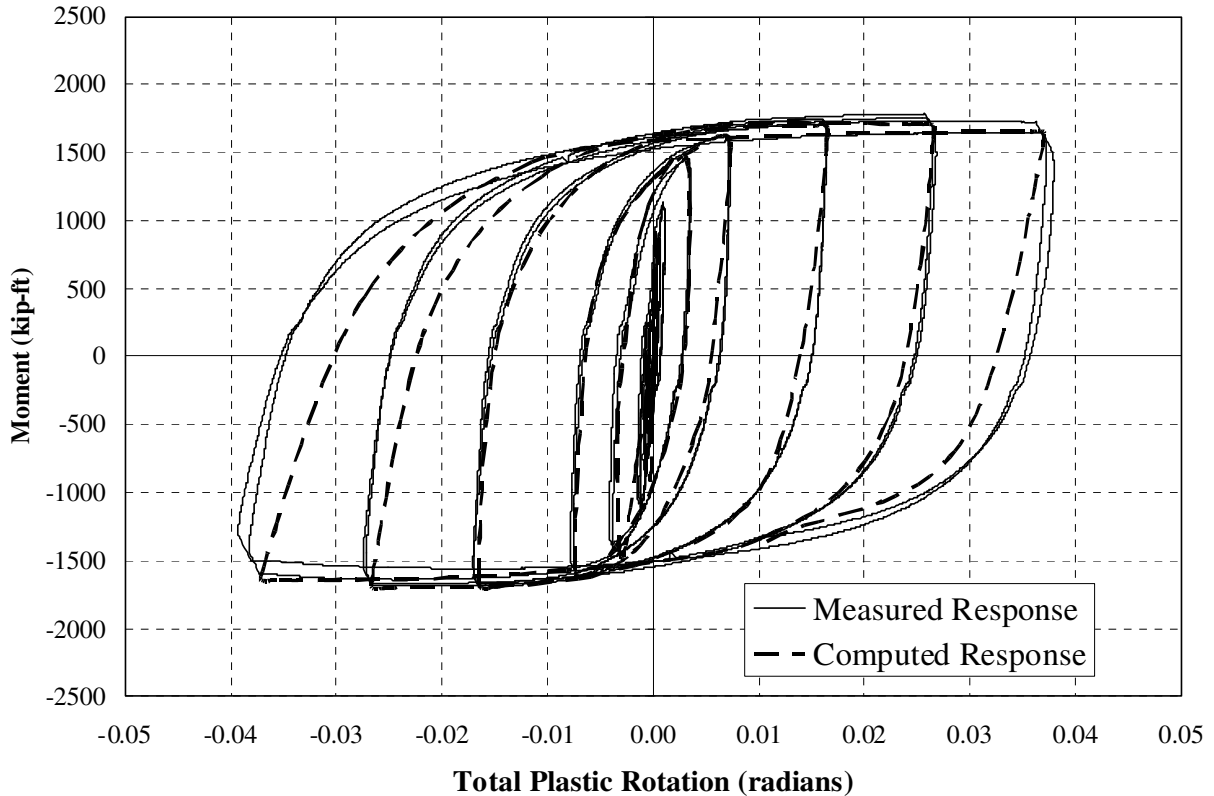
Fig. 10: Comparison between measured moment versus total plastic rotation for the RBS1 (W14x283 column) specimen.
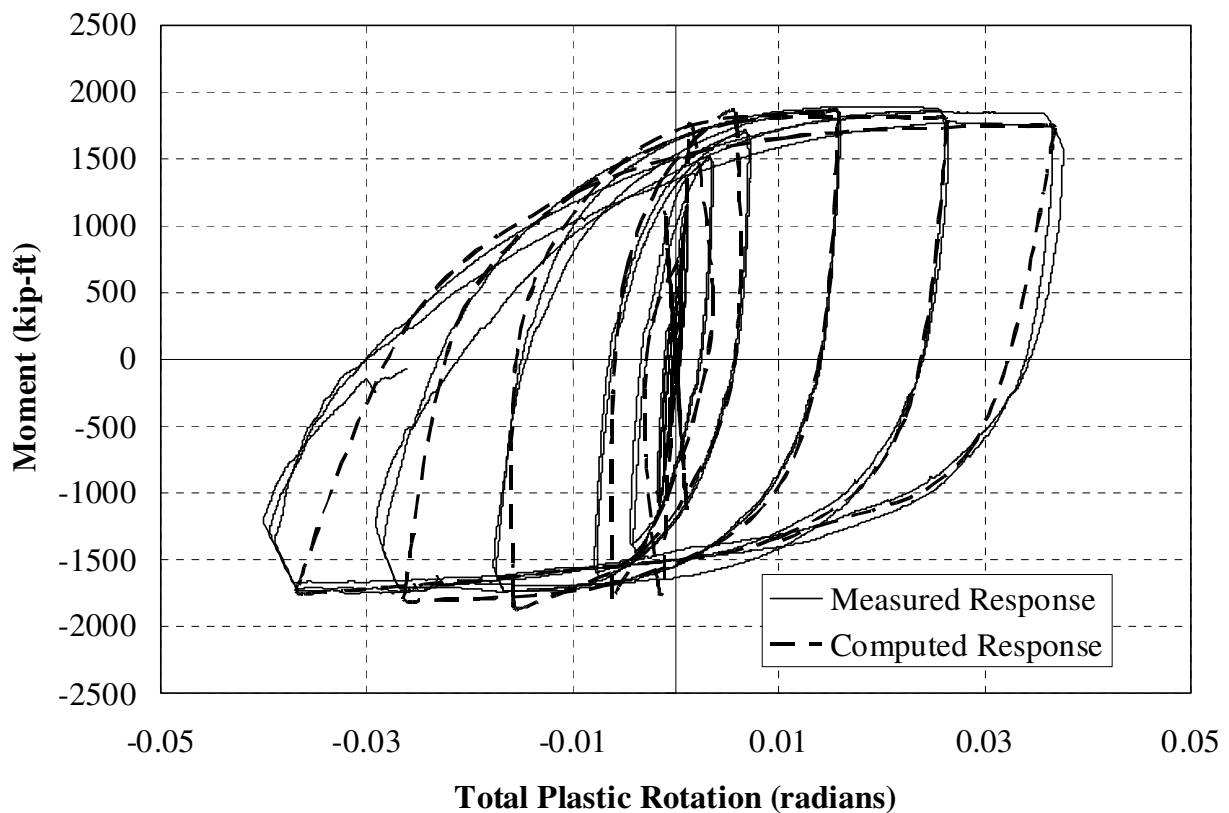
Fig. 11: Comparison between measured moment versus total plastic rotation for the RBS3 (W18x211 column) specimen.

Fig. 10 and 11 indicate that the analytically predicted moment versus plastic rotation response correlates with the response envelope of the test results.

Finite Element Model Behavior

Fig. 12 and 13 show the von Mises stress distributions in the RBS1 (W14x283 column) and the RBS3 (W18x211 column). The figures show the specimens at a downward inter-story drift angle of approximately 0.015 radians. At this angle of rotation no observable signs of buckling were evident during the testing. The connections are approximately at the upper envelop of the elastic state. The dark shaded areas correspond to stress levels of approximately 50.0 to 55.0 ksi. The yielded areas include the beam top and bottom flange at the reduced beam section, the beam web near the reduced beam section, the beam top flange at the column interface, and the column panel zone.
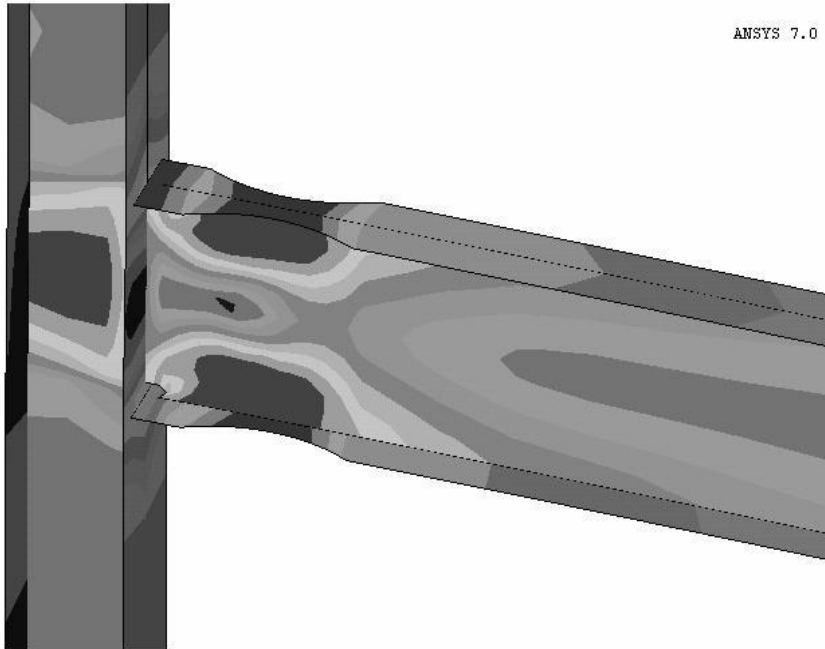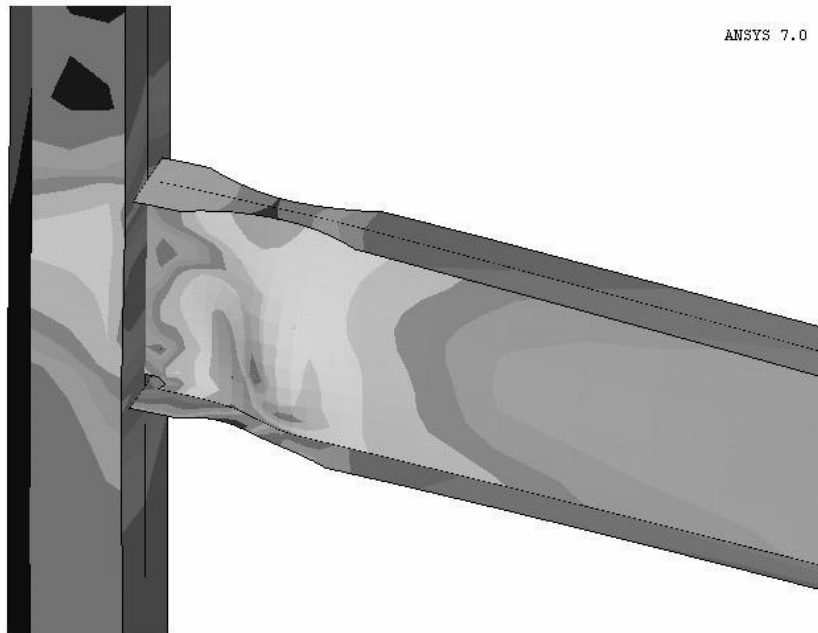
Fig. 12: Oblique deformed view of the von Mises stress distribution in the RBS1 (W14x283 column) specimen at 0.015 radians.
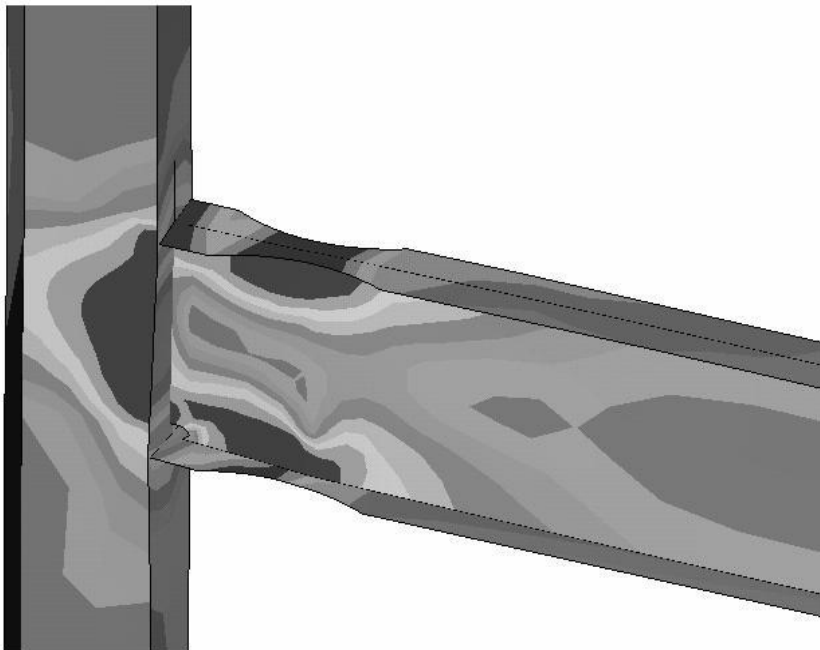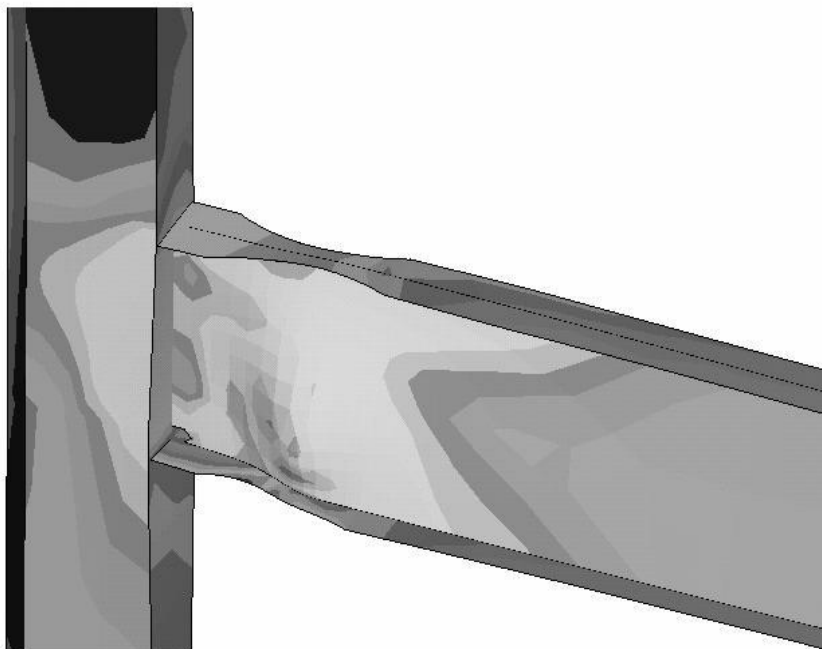

Fig. 13: Oblique deformed view of the von Mises stress distribution in the RBS3 (W18x211 column) specimen at 0.015 radians.

Fig. 14 and 15 show the same specimens at a downward inter-story drift angle of approximately 0.05 radians. This is approximately the upper envelop of the inelastic state and the beams appear to have undergone lateral torsion buckling. The dark shaded areas are at a stress level of approximately 70.0 to 76.0 ksi. These areas include the beam top and bottom flange at the reduced beam section, the beam web

within the reduced beam section. The maximum stress in the column panel zone is approximately 55.0 ksi.

Fig. 14: Oblique deformed view of the von Mises stress distribution in the RBS1 (W14x283 column) specimen at 0.05 radians.

Fig. 15: Oblique deformed view of the von Mises stress distribution in the RBS3 (W18x211 column) specimen at 0.05 radians.

Geometric similarities between the tested section (Fig. 4) and that of the computer generated models (Fig. 14 and 15) tend to validate the methodology used to create the buckled shape. The finite element models

and the tested sections both show similar buckled shapes, and extensive yielding in the reduced beam section. A corresponding moderate zone of yielding is evident in the column panel zone. The shape of the column panel zone stress distribution varies between the W14x283 and W18x211 columns. The column panel zone stress distribution is a subject for further study.

SUMMARY AND CONCLUSIONS

Two RBS beam-to-column nonlinear finite element models were developed to match the four full-scale specimens. The models were used to investigate the behavior of the RBS moment connection without continuity plates. The study involved an exterior connection with a fully restrained, Welded Unreinforced Flange – Welded Web (WUF-W) connection. FEMA 350 [5] pre-qualifies this type of connection for use in Ordinary Moment Frame (OMF) and Special Moment Frame (SMF) systems. The conclusions based on the study are noted below. Further study is necessary to investigate the column panel zone, the behavior of other column sizes, and to develop design recommendations for using the connection without continuity plates:

- The full-scale tests showed that all four specimens exceeded the required inter-story drift requirements for use in SMF systems without continuity plates FEMA 350 [4].
- Finite element modeling can include lateral torsional buckling effects by employing a technique of expanding an eigenvalue buckling analysis into the nonlinear solution of a finite element model.
- Finite element modeling can be correlated to full-scale testing and used as a tool for further investigation into the behavior of the RBS moment connection without continuity plates.
- Elimination of continuity plates in RBS moment connections can provide material and labor cost reductions for steel moment frame construction.

These conclusions have been verified and supported by full-scale inelastic cyclic testing of exterior beam-to-column subassemblies. Currently the authors are continuing study into the column panel zone behavior and the behavior of other column sizes in fully restrained connections. They are also developing design guidelines for using the RBS moment connection without continuity plates.

Acknowledgments

REFERENCES

1. SAC Steel Project. "Protocol for Fabrication, Inspection, Testing, and Documentation of Beam-Column Connection Tests and Other Experimental Specimens." Report No. SAC/BD-97/02, SAC Joint Venture, October 1997.
2. Okahashi Y. "Reduced Beam Section Connection Without Continuity Plates." University of Utah, Salt Lake City, UT, 2003.
3. ANSYS User Manual Version 7.0. ANSYS, Inc., Canonsburg, PA, 2003.
4. Uang CM, Bondad D. "Static Cyclic Testing of Pre-Northridge and Haunch Repaired Steel Moment Connections. Report No. SSRP-96/02, University of California, San Diego, La Jolla, CA, 1996.
5. FEMA 350. "Recommended Seismic Design Criteria For New Steel Moment-Frame Buildings." Federal Emergency Management Agency (FEMA), Washington, D.C., 2000.